The Astrophysical Journal, 650:1111–1118, 2006 October 20
© 2006. The American Astronomical Society. All rights reserved. Printed in U.S.A.

MOST[1] DETECTS g- AND p-MODES IN THE B SUPERGIANT HD 163899 (B2 Ib/II)

H. Saio,[2] R. Kuschnig,[3] A. Gautschy,[4] C. Cameron,[3] G. A. H. Walker,[5] J. M. Matthews,[3] D. B. Guenther,[6] A. F. J. Moffat,[7] S. M. Rucinski,[8] D. Sasselov,[9] and W. W. Weiss[10]

Received 2006 February 23; accepted 2006 June 27

ABSTRACT

The *Microvariability and Oscillations of Stars* (*MOST*) satellite observed the B supergiant HD 163899 (B2 Ib/II) for 37 days as a guide star and detected 48 frequencies $\lesssim 2.8$ cycles day^{-1} with amplitudes of a few millimagnitudes (mmag) and less. The frequency range embraces g- and p-mode pulsations. It was generally thought that no g-modes are excited in less luminous B supergiants because strong radiative damping is expected in the core. Our theoretical models, however, show that such g-modes are excited in massive post–main-sequence stars, in accordance with these observations. The nonradial pulsations excited in models between 20 $M_\odot$ at $\log T_{\rm eff} \approx 4.41$ and 15 $M_\odot$ at $\log T_{\rm eff} \approx 4.36$ are roughly consistent with the observed frequency range. Excitation by the Fe bump in opacity is possible because g-modes can be partially reflected at a convective zone associated with the hydrogen-burning shell, which significantly reduces radiative damping in the core. The *MOST* light curve of HD 163899 shows that such a reflection of g-modes actually occurs and reveals the existence of a previously unrecognized type of variable, slowly pulsating B supergiants (SPBsg) distinct from α Cyg variables. Such g-modes have great potential for asteroseismology.

Subject headings: stars: early-type — stars: individual (HD 163899) — stars: oscillations — supergiants

Online material: color figures

1. INTRODUCTION

The B star region in the H-R diagram contains a wide range of variables. The most luminous (luminosity classes of 0–Ia; $\gtrsim 10^5\ L_\odot$) are known as α Cyg variables and show semiregular light and radial velocity variations on timescales of 1–6 weeks (e.g., van Leeuwen et al. 1998). Those variations are thought to be a combination of pulsation and rotational modulation of winds (e.g., van Genderen 1991; Kaufer et al. 1996, 1997). Pulsations in such very luminous stars can be excited mainly by the Fe bump of opacity (Rogers & Iglesias 1992) at a temperature of about 2×10^5 K. The excitation mechanism is, however, more affected by the strange-mode character in more luminous stars (Kiriakidis et al. 1993; Glatzel & Mehren 1996; Dorfi & Gautschy 2000). The target star discussed in this paper, HD 163899 (B2 Ib/II), is a supergiant that is less luminous and less affected by winds than the α Cyg variables.

There are also many less luminous B-type variable stars whose light and radial velocity variations are caused by radial and nonradial pulsations. These pulsations are excited by the classical κ-mechanism at the Fe bump of opacity. The type of mode excited depends mainly on the effective temperature of the stars; radial and nonradial p-mode pulsations are excited in hotter stars, and nonradial g-mode pulsations are excited in relatively cooler stars (see, e.g., Pamyatnykh 1999). Most of the stars are main-sequence stars. Hotter p-mode pulsators (β Cephei stars) are more luminous or more massive ($\gtrsim 8\ M_\odot$) than the relatively cooler (B3–B8) g-mode pulsators, slowly pulsating B (SPB) stars (Waelkens 1991). Mainly based on line profile variations, g-modes are also known to be excited in early-type Be stars (e.g., Rivinius et al. 2003).

The β Cephei stars have been known for more than a century, but the excitation mechanism was identified only in the early 1990s (Kiriakidis et al. 1992; Moskalik & Dziembowski 1992) after the emergence of OPAL opacity tables (Rogers & Iglesias 1992). The observational properties of the β Cephei stars are thoroughly discussed by Stankov & Handler (2005).

The SPB stars are nearly perfectly confined to the main-sequence band (e.g., De Cat et al. 2004), in accordance with the theoretical prediction that the radiative core in a post–main-sequence star strongly damps g-modes where they have very short wavelengths (Gautschy & Saio 1993; Dziembowski et al. 1993). In this paper, however, we show that reflection of pulsation modes at the convective zone associated with the hydrogen-burning shell quenches the radiative damping in the core, and hence the Fe bump can excite some g-modes in a post–main-sequence massive star with a radiative core.

The *Microvariability and Oscillations of Stars* (*MOST*) photometric satellite was launched on 2003 June and is fully described by Walker et al. (2003). The first scientific results were published by Matthews et al. (2004). *MOST* observations have significantly clarified the properties of pulsating B stars. *MOST* detected clear light variations in the rapidly rotating O9 Ve star ζ Oph (Walker et al. 2005a), which revealed the presence of β Cephei–type pulsations in this line profile variable. *MOST* found

[1] Based on data from the *MOST* satellite, a Canadian Space Agency mission, operated jointly by Dynacon, Inc., the University of Toronto Institute of Aerospace Studies, and the University of British Columbia, with the assistance of the University of Vienna.

[2] Astronomical Institute, Graduate School of Science, Tohoku University, Sendai 980-8578, Japan; saio@astr.tohuku.ac.jp.

[3] Department Physics and Astronomy, University of British Columbia, 6224 Agricultural Road, Vancouver, BC V6T 1Z1, Canada; kuschnig@astro.phys.ubc.ca, matthews@phas.ubc.ca, ccameron@phas.ubc.ca.

[4] Wetterchrüzstrasse 8c, CH-4410 Liestal, Switzerland; alfred@gautschy.ch.

[5] 1234 Hewlett Place, Victoria, BC V8S 4P7, Canada; gordonwa@uvic.ca.

[6] Department of Astronomy and Physics, St. Mary's University, Halifax, NS B3H 3C3, Canada; guenther@ap.stmarys.ca.

[7] Département de Physique, Université de Montréal, C.P. 6128, Succursale Centre-Ville, Montréal, QC H3C 3J7, Canada; and Observatoire du Mont Mégantic, Université de Montréal, Canada; moffat@astro.umontreal.ca.

[8] Department of Astronomy and Astrophysics, David Dunlap Observatory, University of Toronto, P.O. Box 360, Richmond Hill, ON L4C 4Y6, Canada; rucinski@astro.utoronto.ca.

[9] Harvard-Smithsonian Center for Astrophysics, 60 Garden Street, Cambridge, MA 02138; sasselov@cfa.harvard.edu.

[10] Institut für Astronomie, Universität Wien, Türkenschanzstrasse 17, A-1180 Vienna, Austria; weiss@astro.univie.ac.at.

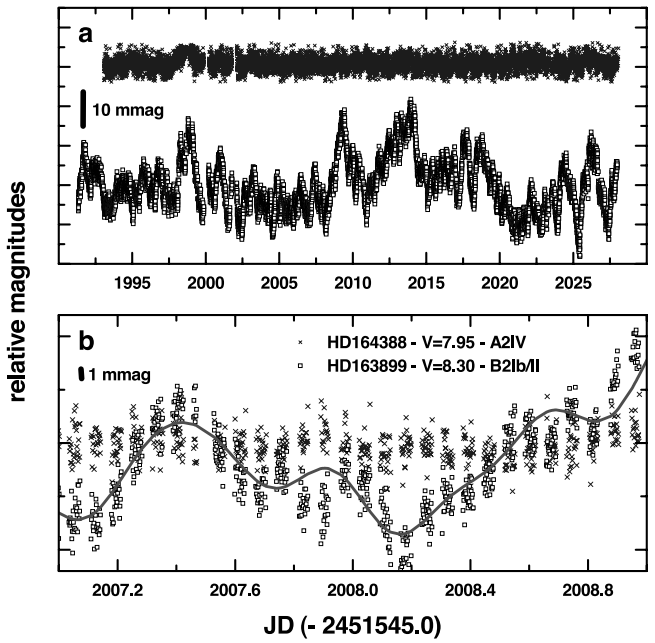

FIG. 1.—(*a*) The 2005 *MOST* 37 day light curve of the guide star HD 163899 and the simultaneously observed guide star HD 164388, whose light curve is shifted by 30 mmag for better visibility. (*b*) A 2 day portion of the HD 163899 light curve with the data binned every 2 minutes. The 2 σ errors are $\sim$1.3 mmag. Because *MOST* was operating outside the continuous viewing zone, the duty cycle was $\sim$50%, accounting for the gaps in the data. The solid line in the bottom panel is the fit of the 48 frequencies detected to the data. A short-term variability of $\sim$0.05 days seen in both stars arose from the orbital phase of the *MOST* satellite and was not included in our frequency search. [*See the electronic edition of the Journal for a color version of this figure.*]

that the monoperiodic β Cephei star δ Ceti is actually multiperiodic, with three additional frequencies (Aerts et al. 2006a). *MOST* discovered a new SPB star, HD 163830 (B5 II/III), near the edge of the main-sequence band, detecting 20 *g*-mode frequencies (Aerts et al. 2006b). *MOST* detected *g*-modes and possibly *r*-modes in the rapidly rotating Be star HD 163868 (Walker et al. 2005b). The latter observations showed, for the first time, that many *g*-modes can be excited in a rapidly rotating Be star and provided a natural interpretation of λ Eri–type variables as SPBe stars. This finding suggests that nonradial pulsations might play a crucial role in Be phenomena. In this paper, we report another important discovery by the *MOST* satellite *g*-modes in the B supergiant HD 163899.

2. THE *MOST* OBSERVATIONS

HD 163899 ($V = 8.3$, B2 Ib/II) was observed as one of 20 guide stars for the photometry of WR 103 (HD 164270) by the *MOST* satellite. The observing conditions and the data reduction method were the same as for the SPBe star HD 163868 described in Walker et al. (2005b). Observations were made from 2005 June 14 to July 21 for a total of 36.6 days with >137,000 values recorded for HD 163899. The data are binned in 2 minute intervals. Since the WR 103 field is outside the *MOST* continuous viewing zone, the duty cycle was limited to about 50% of the 101 minute orbit.

Figure 1 displays the full light curve of HD 163899 and for another guide star, HD 164388 (A2 IV, $V = 8.0$), which appears to be constant (standard deviation $\sim$1.6 mmag). An expanded 2 day portion of the *MOST* light curve is included to better display the higher frequency variations. The light curve shows many periodicities ranging from about a day to a few days, indicating that many *g*-mode pulsations are excited in HD 163899. Complete light curves for both stars can be downloaded from the *MOST* Public Archive.[11]

TABLE 1

HD 163899 PERIODICITIES FROM *MOST* PHOTOMETRY

Number	Frequency (cycles day^{-1})	Amplitude (mmag)	Phase (rad)[a]	S/N
f_1	0.0431 ± 0.0003	4.03 ± 0.08	1.77 ± 0.04	19.2
f_2	0.0726 ± 0.0003	3.00 ± 0.06	3.97 ± 0.04	11.6
f_3	0.0211 ± 0.0009	0.91 ± 0.09	5.12 ± 0.12	10.2
f_4	0.4711 ± 0.0003	2.32 ± 0.03	4.34 ± 0.03	11.9
f_5	0.1911 ± 0.0002	2.37 ± 0.03	6.05 ± 0.02	10.9
f_6	0.2246 ± 0.0003	1.96 ± 0.03	1.48 ± 0.03	11.0
f_7	0.2840 ± 0.0002	1.52 ± 0.06	6.63 ± 0.02	8.5
f_8	0.4009 ± 0.0003	1.69 ± 0.03	1.16 ± 0.04	8.4
f_9	0.6931 ± 0.0009	0.91 ± 0.04	6.68 ± 0.12	7.5
f_{10}	0.5894 ± 0.0007	1.18 ± 0.03	4.80 ± 0.08	7.3
f_{11}	1.0789 ± 0.0003	1.24 ± 0.03	4.90 ± 0.05	7.1
f_{12}	0.1550 ± 0.0004	1.15 ± 0.05	5.68 ± 0.07	7.4
f_{13}	0.1035 ± 0.0006	1.10 ± 0.03	3.14 ± 0.08	6.3
f_{14}	0.3283 ± 0.0003	1.15 ± 0.03	6.86 ± 0.04	6.5
f_{15}	0.9683 ± 0.0011	0.72 ± 0.03	5.25 ± 0.13	6.0
f_{16}	0.6552 ± 0.0006	0.84 ± 0.03	2.32 ± 0.09	5.9
f_{17}	0.4279 ± 0.0006	1.03 ± 0.03	1.64 ± 0.07	6.0
f_{18}	1.9790 ± 0.0004	0.94 ± 0.02	3.11 ± 0.06	6.0
f_{19}	0.3626 ± 0.0006	0.94 ± 0.03	4.06 ± 0.07	5.6
f_{20}	1.3835 ± 0.0006	0.85 ± 0.02	4.52 ± 0.08	5.8
f_{21}	0.5010 ± 0.0008	0.81 ± 0.03	3.25 ± 0.11	5.4
f_{22}	1.1936 ± 0.0005	0.61 ± 0.02	5.18 ± 0.06	5.1
f_{23}	0.8182 ± 0.0005	0.95 ± 0.03	4.60 ± 0.07	5.0
f_{24}	0.2562 ± 0.0006	0.83 ± 0.04	3.29 ± 0.06	5.1
f_{25}	0.8798 ± 0.0009	0.97 ± 0.06	6.62 ± 0.10	5.0
f_{26}	0.7077 ± 0.0011	0.79 ± 0.05	3.41 ± 0.13	5.0
f_{27}	1.3391 ± 0.0010	0.69 ± 0.03	6.38 ± 0.13	4.7
f_{28}	1.4606 ± 0.0008	0.65 ± 0.02	6.34 ± 0.11	4.2
f_{29}	2.0495 ± 0.0004	0.56 ± 0.02	5.80 ± 0.07	4.5
f_{30}	0.8625 ± 0.0011	0.73 ± 0.06	4.86 ± 0.14	4.5
f_{31}	2.2975 ± 0.0010	0.46 ± 0.02	2.29 ± 0.12	4.1
f_{32}	0.9439 ± 0.0011	0.54 ± 0.03	6.74 ± 0.14	4.7
f_{33}	0.7648 ± 0.0009	0.59 ± 0.03	5.37 ± 0.11	4.4
f_{34}	1.6542 ± 0.0016	0.44 ± 0.03	3.20 ± 0.15	3.9
f_{35}	1.1444 ± 0.0007	0.50 ± 0.02	6.39 ± 0.08	4.1
f_{36}	1.9131 ± 0.0010	0.46 ± 0.02	2.28 ± 0.15	4.0
f_{37}	0.5628 ± 0.0016	0.41 ± 0.04	4.53 ± 0.19	3.9
f_{38}	2.5915 ± 0.0009	0.44 ± 0.02	6.93 ± 0.13	4.0
f_{39}	1.5739 ± 0.0008	0.53 ± 0.03	6.96 ± 0.10	4.0
f_{40}	0.1381 ± 0.0008	0.74 ± 0.04	3.63 ± 0.11	4.0
f_{41}	0.3047 ± 0.0004	0.58 ± 0.06	5.46 ± 0.05	3.9
f_{42}	1.3032 ± 0.0011	0.42 ± 0.03	3.69 ± 0.08	4.1
f_{43}	2.3823 ± 0.0007	0.44 ± 0.02	5.93 ± 0.11	4.0
f_{44}	2.8416 ± 0.0010	0.39 ± 0.02	6.54 ± 0.18	4.1
f_{45}	1.7444 ± 0.0014	0.39 ± 0.02	3.31 ± 0.12	3.9
f_{46}	1.5269 ± 0.0014	0.39 ± 0.03	5.52 ± 0.19	3.7
f_{47}	1.6172 ± 0.0014	0.46 ± 0.03	7.17 ± 0.18	3.6
f_{48}	1.0069 ± 0.0018	0.33 ± 0.03	4.23 ± 0.23	3.6

[a] Phases are referenced to the first observation in the data set.

2.1. *The Frequency Analysis*

The frequency analysis was carried out using CAPER, a collection of FORTRAN driver routines that use a discrete Fourier transform (DFT) as a frequency and amplitude identification tool and nonlinear least-squares (NLLS) software (*Numerical Recipes*; Press et al. 1986) to refine the identified parameters. The fitting

[11] The *MOST* Public Archive is available at http://www.astro.ubc.ca/MOST.

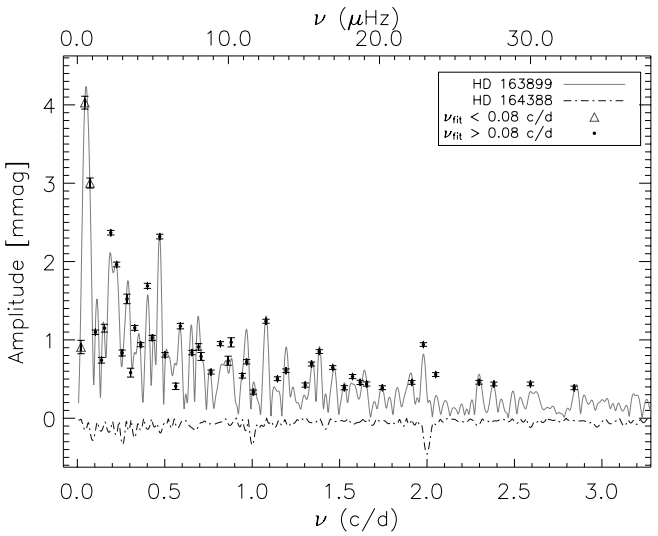

FIG. 2.—Amplitude spectra from discrete Fourier transforms for the light curves of HD 163899 (*solid line*) and the comparison star HD 164388 (*dashed line*), where the sign of the amplitude of the comparison star is inverted for better visibility. Dots and triangles with error bars indicate the frequency/amplitude obtained for HD 163899. Peaks at 1 and 2 cycles day^{-1}, conspicuous in the comparison star, are artifacts typical of the *MOST* photometry. [*See the electronic edition of the Journal for a color version of this figure.*]

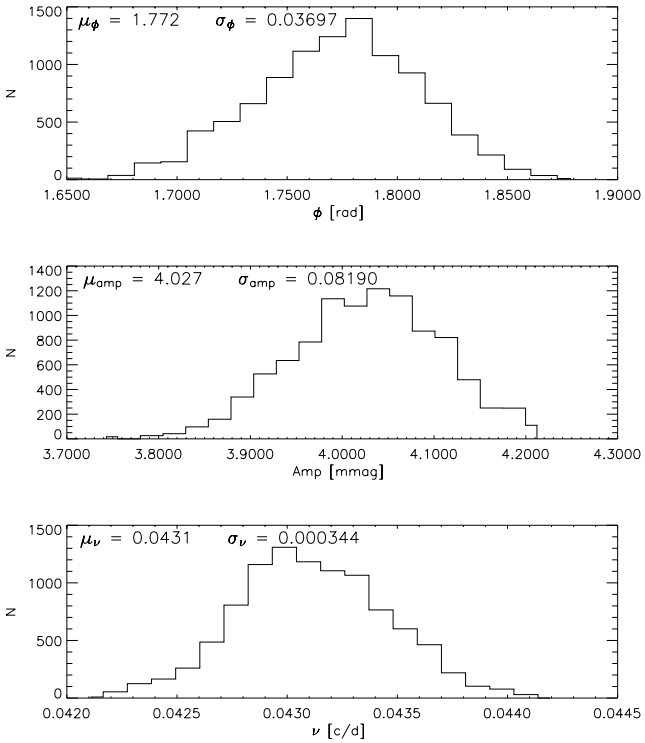

FIG. 3.—Bootstrap distributions of parameters for the frequency f_1. They represent the number of the cases at each parameter bin resulting from 10,000 light curves produced by inserting random gaps into the original. At the top of each diagram the mean value μ and the standard deviation σ of the distribution are indicated. Each diagram from the bottom to the top shows the distribution for the frequency ν in cycles day^{-1}, the amplitude in millimagnitudes, and the phase ϕ in radians.

function is a series of sinusoids (see Walker et al. 2005b). Periodicities were identified and refined as follows.

1. A frequency/amplitude was identified from the DFT. The amplitude and phase were refined via NLLS. The fit function was subtracted from the data, and a new set of parameters was identified from the residuals. The new amplitude and phase was refitted along with all other previously identified amplitudes and phases. The new function was then subtracted from the original time series and new parameters identified. This process is repeated until the next identified frequency has a signal-to-noise ratio (S/N) ~ 3.6 ($\gtrsim 3\ \sigma$ detection; Kuschnig et al. 1997).

Noise is defined as the mean of the amplitude spectrum ± 3 cycles day^{-1} centered on the identified frequency. The amplitudes are 3 σ clipped until the mean converges or until the noise of the entire frequency range is reached. (The frequency range between 0 and 10 cycles day^{-1} has a noise of 0.22 mmag.)

2. Once the 48 frequencies were identified, the three lowest frequencies, along with their amplitudes and phases, were fitted simultaneously by NLLS.

3. The parameters from step (2) were fixed, and all other frequencies, amplitudes, and phases were simultaneously fitted to the original light curve.

We separate the fitting of the parameters in steps (2) and (3) to ensure convergence of the fit. This procedure is similar to low-pass filtering of the data (i.e., removal of as much of the long-term trend as possible before proceeding). The parameters from step (2) are necessary to improve the residuals. The results are presented in Table 1. Figure 2 shows the DFT and the DFT of the comparison star and the fit parameters with bootstrapped errors (described in the following paragraph). The lowest frequency f_3 in Table 1 has a period of 47 days, which is longer than the data and likely to be less accurate.

To assess the precision of our parameter fitting method in steps (2) and (3), we use a bootstrap technique (see, e.g., Wall & Jenkins 2003). The steps (2) and (3) are (separately) repeated 10,000 times with a new light curve that is derived from points randomly selected from the original light curve. The new light curve has the same number of data points as the original, with the possibility that some points may be repeated. This essentially introduces random gaps in the data. Figure 3 shows a typical distribution for a parameter set. The σ of the distribution is used to estimate the 1 σ error bars of each parameter.

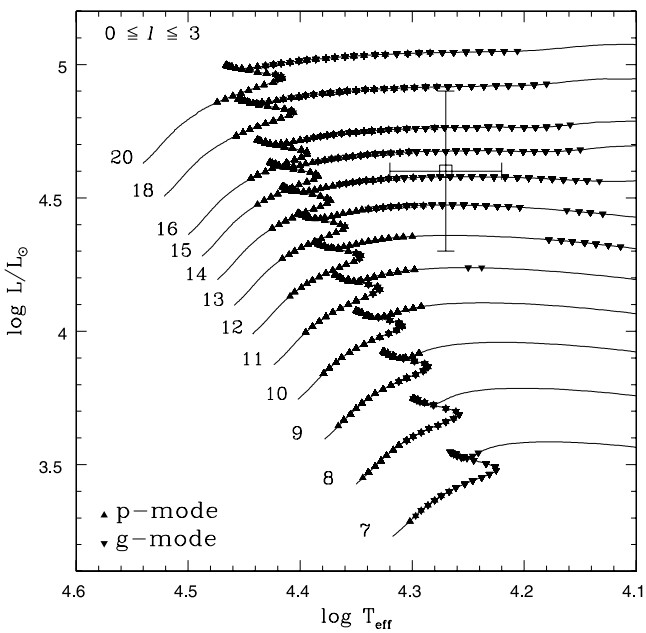

FIG. 4.—Massive star models that excite *p*-modes (*triangles*) and *g*-modes (*inverted triangles*) shown along the evolutionary track for each mass. The models that excite both *g*- and *p*-modes appear as stars. The large square with error bars indicates the position of HD 163899 estimated from the spectral type B2 Ib/II.

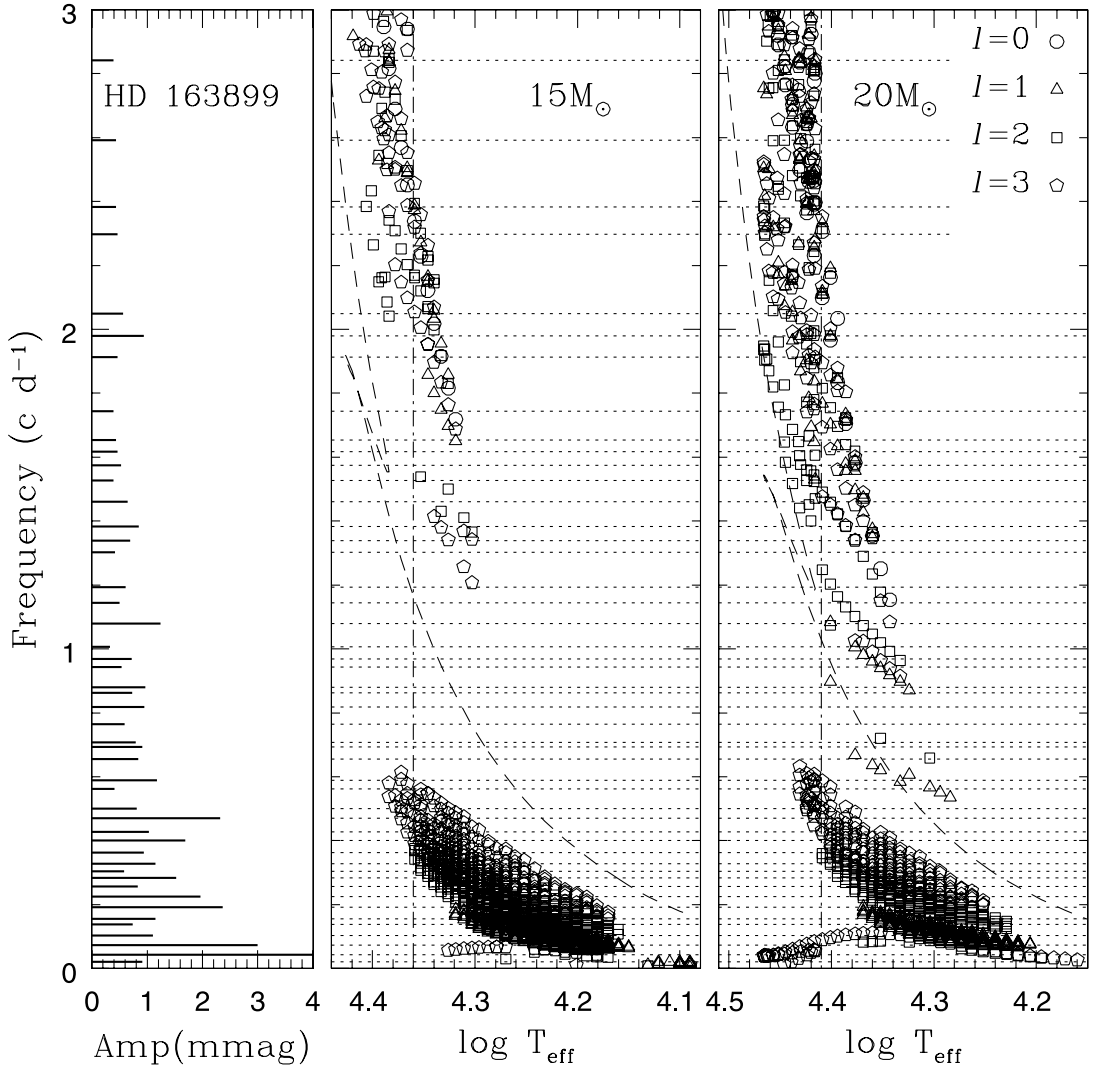

FIG. 5.—Frequencies of excited pulsations of $0 \leq l \leq 3$ in evolutionary models of 15 and 20 $M_{\odot}$ against the effective temperature. The left panel shows frequencies and amplitudes of pulsations obtained by *MOST* for HD 163899. The horizontal dotted lines in the middle and the right panels correspond to the *MOST* frequencies. Long-dashed lines in the middle and right panels indicate the relation of $\sigma = (4\pi G\overline{\rho})^{1/2}$, which is used to discriminate between *p*- and *g*-modes in Fig. 4, where σ is the angular frequency of pulsation, G is the gravitational constant, and $\overline{\rho}$ is the mean density of the star. A vertical dash-dotted line in the middle and right panels indicates a value of $\log T_{\rm eff}$ around which the frequencies excited in the models are roughly consistent with the observed frequencies.

It is reasonable to assume that these multiple periodicities are nonradial pulsations simultaneously excited in the star. The analysis has revealed, in addition to the dense low-frequency spectrum, the presence of relatively high frequencies up to 2.8 cycles day^{-1}, which correspond to *p*-mode pulsations (i.e., both *p*- and *g*-modes are excited simultaneously in HD 163899). To the authors' knowledge, it is the first clear detection of *g*-modes in a less luminous B supergiant, although Waelkens et al. (1998)'s list of the *Hipparcos* α Cyg–type supergiants contains some less luminous supergiants with periods of a few days, indicating the possible presence of *g*-modes.

3. MODELING THE OSCILLATIONS

To examine the stability of post–main-sequence models corresponding to B supergiants and bright giants, we have computed evolution models for a mass range of $7 \leq M/M_{\odot} \leq 20$ with an initial chemical composition of $(X, Z) = (0.7, 0.02)$. We used a Henyey-type stellar evolution code with OPAL opacities (Iglesias & Rogers 1996). The stability of nonradial pulsations has been examined for selected models by using a finite difference method (Saio & Cox 1980). The stability of a selected model has also been analyzed with a Riccati shooting code (Gautschy et al. 1996). We have confirmed that the results of the two methods agree well.

Figure 4 shows positions of models in the H-R diagram that excite *p*-modes (*triangles*) and *g*-modes (*inverted triangles*). (The models that excite both *g*- and *p*-modes appear as stars.) If the angular frequency of pulsation is larger (smaller) than $(4\pi G\overline{\rho})^{1/2}$, the mode is classified as a *p*-mode (*g*-mode), where G and $\overline{\rho}$ are the gravitational constant and the mean density of the model (see also Fig. 5). The *p*-mode (β Cephei–type) instability range and the usual SPB *g*-mode instability range for main-sequence stars of $M \lesssim 9\ M_{\odot}$ agree with those obtained by Pamyatnykh (1999). We also note that the red edge of the radial mode instability range of 20 $M_{\odot}$ models is located at $\log T_{\rm eff} = 4.34$, in perfect agreement with the result of Kiriakidis et al. (1993), who examined the stability of radial modes for very massive stars.

In addition to the known instability regions, Figure 4 shows a wide *g*-mode instability region for the post–main-sequence massive ($M \gtrsim 12\ M_{\odot}$) models. The instability region has not been recognized before. In fact, the stability of *g*-modes in the post–main-sequence massive stars had not been examined since the

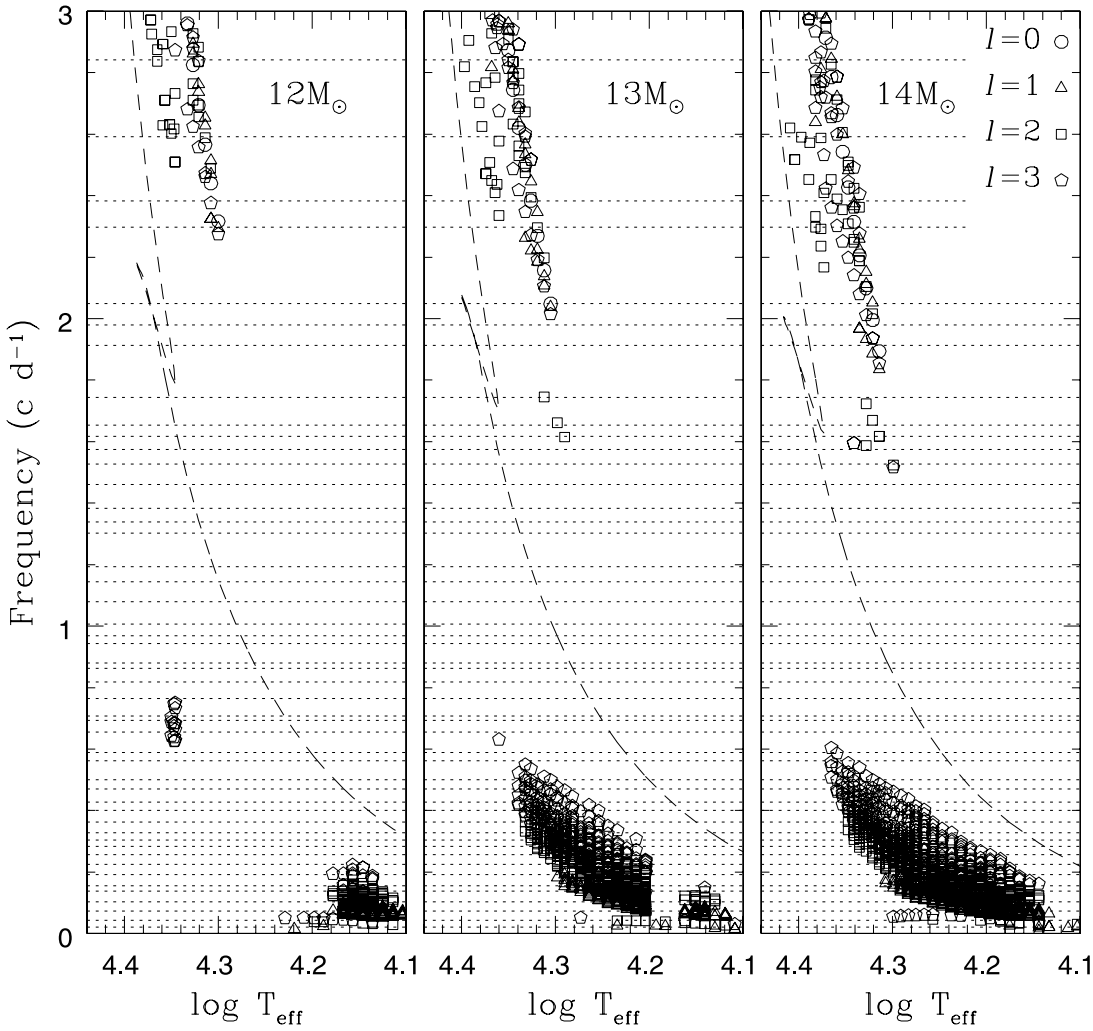

FIG. 6.—Frequencies of excited pulsations of $0 \leq l \leq 3$ in evolutionary models of 12, 13, and 14 $M_\odot$ against the effective temperature. The dashed lines and dotted lines are the same as in Fig. 5.

emergence of OPAL opacities. (Glatzel & Mehren [1996] examined the stability of p-modes, but not of higher order g-modes.) In § 4, we focus on the properties of unstable high-order g-modes.

In the hotter part of the instability region, p-modes are also excited simultaneously. The position of HD 163899 shown in Figure 4, which is roughly estimated from its spectral type B2 Ib/II, indicates that HD 163899 lies in the newly found instability region. In other words, HD 163899 belongs to a previously unrecognized type of pulsating stars, which we call "slowly pulsating B supergiants" (or SPBsg). Strictly speaking, HD 163899, showing both g- and p-modes, is a hybrid of SPBsg and β Cephei type.

Figure 5 shows pulsation frequencies (cycles per day) of excited modes versus effective temperature along the evolutionary tracks of 15 and 20 $M_\odot$. The left panel shows each frequency and amplitude of the periodicities of HD 163899 detected by the *MOST* satellite. The horizontal dotted lines in the middle and the right panels correspond to the *MOST* frequencies. The dashed lines show the frequency given by $(4\pi G\overline{\rho})^{1/2}/(2\pi)$ along the evolutionary track. This line is used to distinguish between p- and g-modes in Figure 4. Figure 6 shows similar plots for 12, 13, and 14 $M_\odot$.

P-modes are excited in hotter models, while g-modes are excited in relatively cooler ones. The frequencies of the excited g-modes tend to be higher for a larger latitudinal degree l. In restricted $T_{\rm eff}$ ranges, both p-modes and g-modes are excited simultaneously, and the corresponding models are appropriate for HD 163899. Since a linear stability analysis cannot predict the amplitudes of unstable modes, we compare in this first attempt only the predicted frequency ranges of excited modes with the observed ones. The observed frequency range is reproduced by the 20 $M_\odot$ models around $\log T_{\rm eff} \sim 4.41$ and by the 15 $M_\odot$ models $\log T_{\rm eff} \sim 4.36$. (These are indicated by vertical dash-dotted lines in Fig. 5.) On the other hand, for 14 and 13 $M_\odot$ models the frequency gap between p- and g-modes looks too large to be consistent with the observed frequency distribution.

Taking into account that the estimated range of $\log T_{\rm eff}$ for B2 Ib/II is roughly between 4.22 and 4.32 (Fig. 4), a 15 $M_\odot$ model at $\log T_{\rm eff} \approx 4.36$ looks best to reproduce the observed frequency range of HD 163899. Although the frequency gap is still large, it would be filled, at least partially, by rotational splittings. (If a higher $T_{\rm eff}$ is allowed, 20 $M_\odot$ models at $\log T_{\rm eff} \approx 4.41$ work better.)

In our models, rotation is completely disregarded. In the presence of rotation, a pulsation frequency measured in the observer's frame, ν(obs), shifts as

$$\nu(\text{obs}) = \nu(\text{rot}) - m\Omega, \tag{1}$$

from the frequency in the corotating frame, ν(rot), where m is the azimuthal order ($|m| \leq l$) and Ω is the rotation frequency.

If we assume that HD 163899 rotates at a speed of about 100 km s^{-1}, an average for B2 Ib/II (Abt et al. 2002), the rotation frequency would be $\approx$0.1 cycles day^{-1}. If we assume $l \leq 3$ for observed pulsation modes, we expect that observed frequencies would be shifted by at most $\approx \pm 0.3$ cycles day^{-1} from ν(rot)s, which we assume to be close to those obtained for $\Omega = 0$. This effect would nearly fill the frequency gap between p- and g-modes, and make the predicted frequency distribution roughly consistent with the observed one for HD 163899.

It is not possible to perform a detailed comparison between the detected frequencies and theoretical predictions until accurate information on the parameters of HD 163899, such as effective temperature, luminosity, and rotation speed, is available. The most important finding in our modeling exercises is the fact that g-modes can be excited in post–main-sequence models, which suggests the presence of a new group of variable stars. We discuss, in § 4, the properties of excited g-modes.

Figures 4 and 5 indicate that earlier B supergiants should pulsate in p-modes. This theoretical prediction is consistent with the recent observational result of Kaufer et al. (2006), who detected short-period line profile variations in HD 64760 (B0.5 Ib).

Before we proceed to § 4, we note that there are strongly excited very low frequency modes, which are most clearly seen as a lowest frequency branch in the frequency-$T_{\rm eff}$ diagram for 20 $M_\odot$ in Figure 5. The amplitude of these modes is strongly confined to the exterior of the bottom of the Fe convection zone. The frequencies are so low that these modes are propagative even at the outer boundary. Since we use a reflective boundary condition at the outer boundary, we do not regard the stability of these modes to be accurate. In addition, the property of these modes would be modified significantly in the presence of slow rotation. Therefore, we have not included these modes in Figure 4. We leave these modes for future investigations.

4. EXCITATION OF g-MODES

We have found that g-modes are excited in massive post–main-sequence stars, whose central part is in radiative equilibrium. This looks contrary to the general thought that g-modes should be damped due to very strong dissipation expected in a radiative core where the Brunt-Väisälä frequency is very high. The excitation becomes possible, however, due to the presence of a fully developed convective shell associated with the hydrogen-burning shell in a massive star. (Fully developed convection means that convective mixing is strong enough to homogenize the chemical composition.) Since a g-mode pulsation is evanescent in the convection zone, it can be reflected at the boundary. In other words, the convective shell can prevent a g-mode from penetrating into the radiative core.

Figure 7 shows runs of Lamb frequency, $L_l^2 = l(l+1)c_s^2 r^{-2}$, and Brunt-Väisäla frequency, N^2, which is approximately written for an ideal gas as

$$N^2 \approx \frac{g}{H_p}\left[\left(\frac{d\ln T}{d\ln P}\right)_{\rm ad} + \left(\frac{d\ln \mu}{d\ln P}\right) - \left(\frac{d\ln T}{d\ln P}\right)\right], \quad (2)$$

where c_s is the adiabatic sound speed, r is the distance from the stellar center, g is the local gravity, H_p is the pressure scale height, P is the pressure, and μ is the mean molecular weight. Frequencies of excited g-modes of $l = 2$ are shown by dotted horizontal lines. In this figure all quantities are normalized by GMR^{-3}.

Roughly speaking, the radial wavenumber of a g-mode that pulsates with an angular frequency σ is proportional to $\sigma^{-1}[(N^2 - \sigma^2)(L_l^2 - \sigma^2)]^{1/2}$. Therefore, g-modes are radially propagative only if $\sigma^2 < N^2$ and $\sigma^2 < L_l^2$, and evanescent otherwise (see, e.g., Unno et al. [1989] and Cox [1980] for details). Since both N^2 and L_l^2 are very large in the radiative core, we expect a very large wavenumber (i.e., very short wavelength) and hence a large radiative damping for a g-mode in the central part. This is the reason why we do not generally expect g-modes to be excited in a post–main-sequence star with a radiative nondegenerate core.

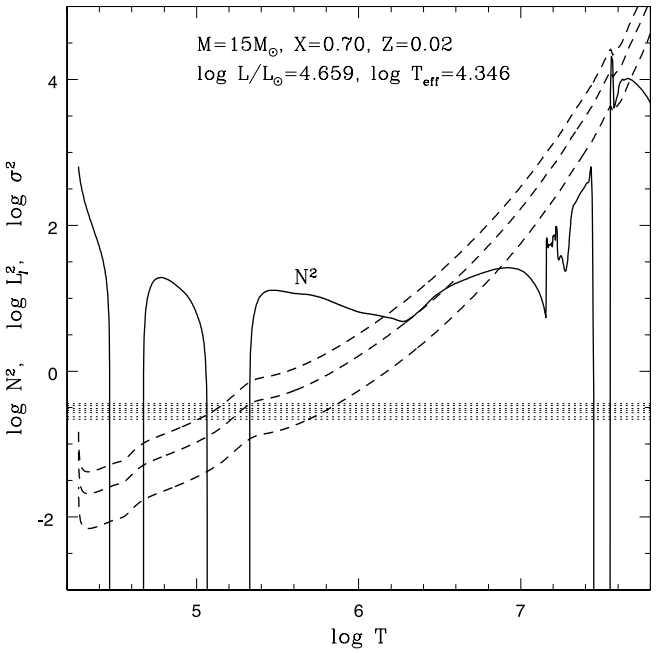

FIG. 7.—Runs of the square of the Brunt-Väisälä frequency, N^2, and the square of Lamb frequency, $L_l^2 = l(l+1)c_s^2/r^2$, for $l = 1, 2, 3$. Horizontal dotted lines indicate the angular frequencies (σ) of g-modes of $l = 2$ excited in this model. All the quantities in this figure are normalized by GMR^{-3}.

In a massive post–main-sequence star, however, a fully developed convection zone appears at the hydrogen-burning shell, which is seen as a narrow gap around $\log T \sim 7.5$ in Figure 7. This zone, where g-modes are evanescent, can reflect some g-modes and prevent them from penetrating into the core. This effect reduces radiative damping in the core significantly and hence helps the κ-mechanism in the envelope excite the mode.

Figure 8 shows the work W, differential work $dW/d(-\log T)$, radial displacement amplitude, and kinetic energy distribution (*top*) of an excited g-mode. The pulsation is excited if the value of W is positive at the surface. [The differential work $dW/(-d\log T) > 0$ means that the zone drives pulsation.] We see that the amplitude and kinetic energy suddenly becomes very small interior to the point at $\log T \approx 7.5$, where the fully convective zone is located. This indicates that the reflection at the convective shell actually occurs for this mode. Such a reflection at the convective shell is essential for a g-mode to be excited in a post–main-sequence star by the κ-mechanism at the Fe bump of opacity. All post–main-sequence models that excite g-modes in Figure 4 have a fully developed convection zone associated with the hydrogen-burning shell. On the other hand, in a stable range of $4.16 \lesssim \log T_{\rm eff} \lesssim 4.20$ for 13 $M_\odot$ (Fig. 6), for example, no fully developed convective zone is present at the hydrogen-burning shell (i.e., the whole convectively unstable layers are semiconvective only).

Only a few selected g-modes are reflected at the convection zone and excited by the Fe bump in an appropriate frequency range. Figure 9 compares the kinetic energy distribution of an excited $l = 2$ g-mode (*thick solid line*) to that of a damped mode

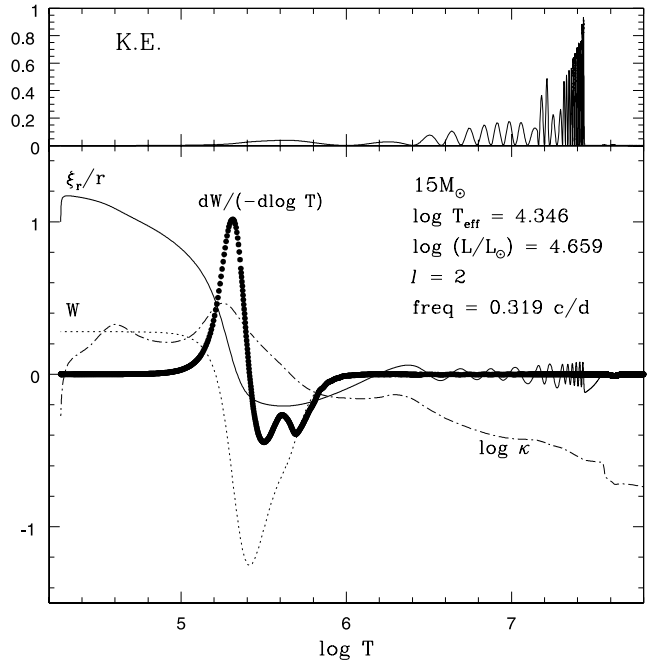

FIG. 8.—*Bottom*: Radial displacement (*solid line*), work W (*dotted line*), differential work $dW/(-d \log T)$ (*dots*), and opacity κ (*dash-dotted line*) as a function of $\log T$. *Top*: Distribution of the kinetic energy of the pulsation. Radiative dissipation in the core is quenched because the pulsation is reflected at the convective shell at $\log T \approx 7.5$. The opacity peak at $\log T \approx 5.3$ arises from Fe, and that at $\log T \approx 4.6$ arises from He II ionization.

(*thin solid line*) as a function of the fractional radius ($x = r/R$). (In this diagram the right-hand side is the stellar surface.) The pulsation frequencies of the two modes are very close: 0.324 and 0.326 cycles day^{-1}. These eigenfunctions were calculated by the Riccati shooting method (Gautschy et al. 1996), completely resolving the spatial oscillations with roughly 16,500 integration steps. It is obvious that the kinetic energy in the core of the excited mode is significantly reduced, and hence the radiative damping is quenched, while the kinetic energy of the damped mode is strongly confined to the central part.

Most of the g-modes in the frequency range where excited modes reside are confined to the radiative core and are damped due to strong radiative damping. Only those selected g-modes whose spatial oscillations have the right phase at the boundary of the chemically homogeneous shell convection zone are reflected and confined to the envelope. Therefore, which g-modes are excited depends on details of the structure around the convective shell. In the model shown in Figure 7, the layer in $7.23 \leq \log T \leq 7.44$ is semiconvective (i.e., convective zone with an inhomogeneous chemical composition). We have treated semiconvective mixing based on the model of Spruit (1992). Everyone admits that many uncertainties lie in the theory of convective mixing. Since the Brunt-Väisälä frequency depends sensitively on the distribution of chemical elements (eq. [2]), frequency spacings of the excited g-modes depend on the treatment of convective mixing. This indicates that comparing observed frequencies with the predicted ones from models can constrain the theory of convective mixing. We also note that the lower luminosity boundary of the g-mode instability region, which is the boundary of the presence of a fully developed shell convection, depends on the efficiency of convective mixing. Thus, g-modes in SPBsgs have great potential for asteroseismology.

As discussed above, the presence of a convective shell is crucial to excite g-modes in the post–main-sequence models. The

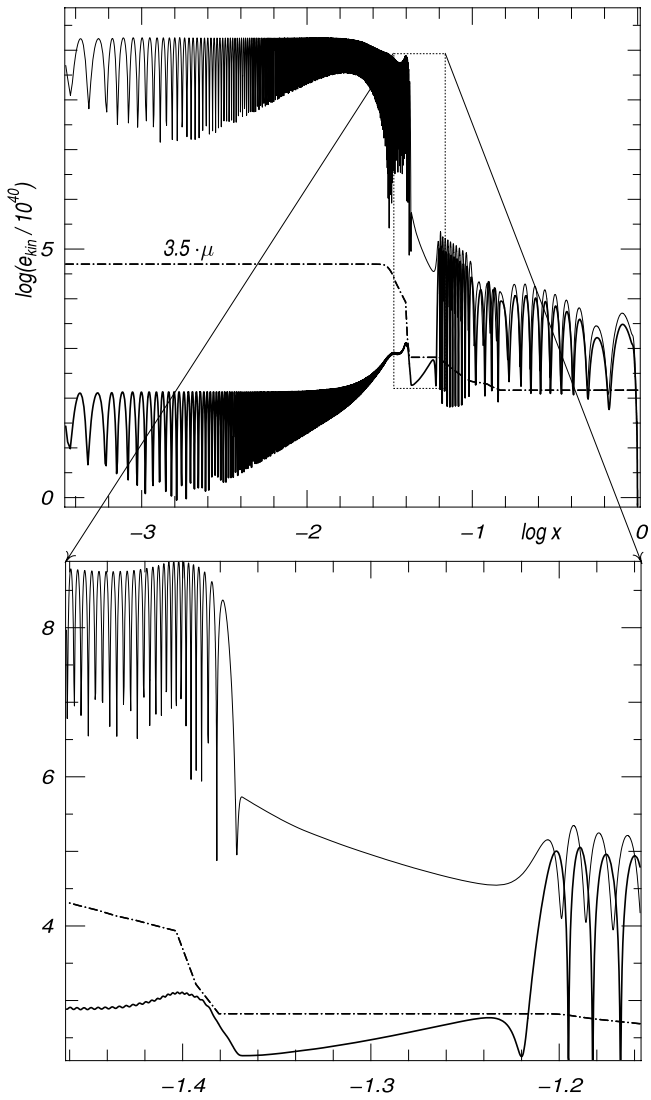

FIG. 9.—Kinetic energy distribution of an excited 0.3241 cycles day^{-1} mode (*thick solid lines*) and a damped 0.3256 cycles day^{-1} mode (*thin solid lines*) of $l = 2$ as a function of the fractional distance from the center ($x = r/R$). (The thin line is the upper one.) Dot-dashed lines show the suitably scaled spatial variation of the mean molecular weight. The kinetic energy of the excited mode is very small in the core due to the reflection in the convective shell, which reduces radiative damping in the core and hence makes the mode unstable.

appearance of a convective shell in the post–main-sequence phase of massive stars has been known for more than 30 years (e.g., Barbaro et al. 1972). It has also been known for a long time that g-modes can be reflected at the boundary of a convection zone and that the reflection quenches a strong radiative dissipation in the core. Nevertheless, we can find no published evidence of stability analyses of g-modes in massive post–main-sequence stars since the emergence of OPAL opacities. The discovery of light variations in HD 163899 by the *MOST* satellite, which prompted us to perform stability analyses for such modes, played a crucial role in our eventually finding the excited high-order g-modes. On the H-R diagram, the region with unstable g-modes seems to extend to the region of α Cyg variables, suggesting that g-mode pulsations might play an important role in understanding these luminous variable stars. The spatiotemporal evolution of the H-shell convection zone in very massive stars during their post–main-sequence evolution can be judged from figures in, e.g., Lamb et al. (1976) or Maeder (1981).

5. CONCLUSION

The *MOST* satellite discovered that the B-type supergiant HD 163899 pulsates in g-modes as well as in p-modes, showing, for the first time, SPB-type g-mode pulsations in a less luminous B supergiant. We have performed pulsation stability analyses for evolutionary models in the mass ranges of $7 \leq M/M_{\odot} \leq 20$ and found that g-modes are excited by the Fe bump of opacity in post–main-sequence stars in a wide range of effective temperatures if the stellar mass is larger than $\sim$12 $M_{\odot}$. Our results indicate the existence of a previously unrecognized group of variable stars: slowly pulsating B supergiants (SPBsg) distinct from α Cyg variables.

The excitation of g-modes in B supergiants becomes possible by a reflection of g-modes at the fully developed convection zone associated with the hydrogen-burning shell. This reduces significantly the radiative damping in the radiative core of the star. Since the frequencies of excited g-modes depend on the structure around the convective shell, SPBsg stars have a great potential for asteroseismology.

HD 163899 is the first member of the SPBsg family. Strictly speaking, HD 163899, showing both g- and p-modes, is a hybrid of SPBsg and β Cephei type. The B supergiant ι CMa (B3 Ib/II) could be another SPBsg member. Balona & Engelbrecht (1985) obtained a 0.717 cycles day^{-1} periodicity for ι CMa. Since the light curve looks irregular, it is likely multiperiodic. Another possible candidate could be HD 98410 (B2/B3 Ib/II), which is listed in Stankov & Handler (2005) as one of the "poor and rejected β Cephei candidates" with a *Hipparcos*-deduced period of 1.453 days. We also note that Waelkens et al. (1998)'s list for α Cyg–type supergiants includes some less luminous B supergiants or bright giants such as HD 54764 (B1 Ib/II), HD 141318 (B2 II), and HD 168183 (B1 Ib/II). These stars could also be SPBsg candidates. Further observations of these stars are needed to confirm their membership. In addition, for a detailed asteroseismological study of HD 163899, spectroscopic observations are important to properly identify the pulsation modes that are responsible for the photometrically observed frequencies.

This research has made use of the SIMBAD database, operated at CDS, Strasbourg, France. The Natural Sciences and Engineering Research Council of Canada supports the research of D. B. G., J. M. M., A. F. J. M., S. M. R., E. S., and G. A. H. W. A. F. J. M. is also supported by Le Fonds Québécois de la Recherche sur la Nature et les Technologies (FQRNT) of Québec. R. K. is supported by the Canadian Space Agency. W. W. W. is supported by the Austrian Space Agency and the Austrian Science Fund (P14984). H. S. is supported by the 21st Century Center of Excellence (COE) program of the Ministry of Education, Culture, Sports, Technology and Science (MEXT), Japan.

REFERENCES

Abt, H. A., Levato, H., & Grosso, M. 2002, ApJ, 573, 359
Aerts, C., et al. 2006a, ApJ, 642, 470
———. 2006b, ApJ, 642, L165
Balona, L. A., & Engelbrecht, C. A. 1985, MNRAS, 214, 559
Barbaro, G., Chiosi, C., & Nobili, L. 1972, A&A, 18, 186
Cox, J. P. 1980, Theory of Stellar Pulsation (Princeton: Princeton Univ. Press), 251
De Cat, P., et al. 2004, in IAU Colloq. 193, Variable Stars in the Local Group, ed. D. W. Kurtz & K. R. Pollard (ASP. Conf. Ser. 310; San Francisco: ASP), 195
Dorfi, E. A., & Gautschy, A. 2000, ApJ, 545, 982
Dziembowski, W. A., Moskalik, P., & Pamyatnykh, A. A. 1993, MNRAS, 265, 588
Gautschy, A., Ludwig, H.-L., & Freytag, B. 1996, A&A, 311, 493
Gautschy, A., & Saio, H. 1993, MNRAS, 262, 213
Glatzel, W., & Mehren, S. 1996, MNRAS, 282, 1470
Iglesias, C. A., & Rogers, F. J. 1996, ApJ, 464, 943
Kaufer, A., Stahl, O., Prinja, R. K., & Witherick, D. 2006, A&A, 447, 325
Kaufer, A., Stahl, O., Wolf, B., Gäng, T., Gummersbach, C. A., Kovács, J., Mandel, H., & Szeifert, T. 1996, A&A, 305, 887
Kaufer, A., et al. 1997, A&A, 320, 273
Kiriakidis, M., El Eid, M. F., & Glatzel, W. 1992, MNRAS, 255, 1P
Kiriakidis, M., Fricke, K. J., & Glatzel, W. 1993, MNRAS, 264, 50
Kuschnig, R., Weiss, W. W., Gruber, R., Bely, P. Y., & Jenkner, H. 1997, A&A, 328, 544
Lamb, S. A., Iben, I., & Howard, W. M. 1976, ApJ, 207, 209
Maeder, A. 1981, A&A, 99, 97
Matthews, J. M., Kusching, R., Guenther, D. B., Walker, G. A. H., Moffat, A. F. J., Rucinski, S. M., Sasselov, D., & Weiss, W. W. 2004, Nature, 430, 51
Moskalik, P., & Dziembowski, W. A. 1992, A&A, 256, L5
Pamyatnykh, A. A. 1999, Acta Astron., 49, 119
Press, W. H., Flannery, B. P., Teukolsky, S. A., & Vetterling, W. T. 1986, Numerical Recipes (Cambridge: Cambridge Univ. Press), 498
Rivinius, Th., Baade, D., & Štefl, S. 2003, A&A, 411, 229
Rogers, F. J., & Iglesias, C. A. 1992, ApJS, 79, 507
Saio, H., & Cox, J. P. 1980, ApJ, 236, 549
Spruit, H. C. 1992, A&A, 253, 131
Stankov, A., & Handler, G. 2005, ApJS, 158, 193
Unno, W., Osaki, Y., Ando, H., Saio, H., & Shibahashi, H. 1989, Nonradial Oscillations of Stars (Tokyo: Univ. Tokyo Press), 114
van Genderen, A. M. 1991, in ESO Workshop on Rapid Variability of OB-Stars: Nature and Diagnostic Value, ed. D. Baade (Garching bei Munich: ESO), 117
van Leeuwen, F., van Genderen, A. M., & Zegelaar, I. 1998, A&AS, 128, 117
Waelkens, C. 1991, A&A, 246, 453
Waelkens, C., Aerts, C., Kestens, E., Grenon, M., & Eyer, L. 1998, A&A, 330, 215
Walker, G. A. H., et al. 2003, PASP, 115, 1023
———. 2005a, ApJ, 623, L145
———. 2005b, ApJ, 635, L77
Wall, J. V., & Jenkins, C. R. 2003, Practical Statistics for Astronomers (Cambridge: Cambridge Univ. Press), 130